A novel independence test for somatic alterations in cancer shows that biology drives mutual exclusivity but chance explains co-occurrence

Sander Canisius[1], John W.M. Martens[2], and Lodewyk F.A. Wessels[1,3]

[1]*Department of Molecular Carcinogenesis, The Netherlands Cancer Institute, Amsterdam, The Netherlands*
[2]*Department of Medical Oncology, Erasmus University Medical Center, Rotterdam, The Netherlands*
[3]*Faculty of EEMCS, Delft University of Technology, Delft, The Netherlands*

Abstract

Just like recurrent somatic alterations characterize cancer genes, mutually exclusive or co-occurring alterations across genes suggest functional interactions. Identifying such patterns in large cancer studies thus helps the discovery of unknown interactions. Many studies use Fisher's exact test or simple permutation procedures for this purpose. These tests assume identical gene alteration probabilities across tumors, which is not true for cancer. We show that violating this assumption yields many spurious co-occurrences and misses many mutual exclusivities. We present DISCOVER, a novel statistical test that addresses the problems with common tests. A pan-cancer analysis using DISCOVER finds no evidence for widespread co-occurrence. Most co-occurrences previously detected do not exceed expectation by chance. In contrast, many mutual exclusivities are identified. These cover well known genes involved in the cell cycle and growth factor signaling. Interestingly, also lesser known regulators of the cell cycle and Hedgehog signaling are identified.

Availability: R and Python implementations of DISCOVER, as well as Jupyter notebooks for reproducing all results and figures from this paper can be found at `http://ccb.nki.nl/software/discover`.

1 Introduction

Tumor development emerges from a gradual accumulation of somatic alterations that together enable malignant growth. As has been revealed by recent genomic profiling efforts, an immense diversity exists in the alterations that tumors acquire (Vogelstein et al. 2013; Lawrence et al. 2014). Whether by e.g. copy number aberration, point mutation, or DNA methylation, alterations of many genes may potentially trigger transformation. Often though, the fate of a cell acquiring a certain alteration depends on other alterations already present (Ashworth et al. 2011). Therefore, with an ever-expanding catalog of cancer genes, a need arises to establish how alterations in those genes interact to transform healthy cells to cancer cells. This task can be approached by statistical analyses aiming to uncover more complex, combinatorial patterns in somatic alterations.

Two such patterns are co-occurrence and mutual exclusivity. In the former, a group of genes tends to be altered simultaneously in the same tumor, whereas in the latter, mostly only one out of a group of genes is altered in a single tumor. Mutual exclusivity is frequently observed in cancer genomics data (Thomas et al. 2007; Yeang et al. 2008). Individual alterations targeting similar biological processes are believed to be mutually redundant, with one alteration being sufficient to deregulate the affected process. Identifying mutual exclusivity can therefore help in finding unknown functional interactions. With this in mind, several statistical methods have been proposed to identify significant patterns of mutual exclusivity (Ciriello et al. 2012; Vandin et al. 2012; Szczurek and Beerenwinkel 2014).

Just as mutual exclusivity is interpreted as a sign of redundancy, co-occurrence is often held to entail synergy. Alteration of only one of the two genes would be relatively harmless, whereas cells with alterations in both progress to malignancy. If such synergy exists, cancer genomes should be enriched for these co-alterations, i.e. tumors harboring alterations in both genes should be more frequent than expected by chance. Several studies have reported an abundance of co-occurring somatic alterations in various types of cancer (Bredel et al. 2009; Gorringe et al. 2010; Klijn et al. 2010; Milosevic et al. 2012; Kandoth et al. 2013; Remy et al. 2015). For somatic copy number changes, however, it has also been suggested that co-occurring alterations emerge from tumors' overall levels of genomic disruption (Zack et al. 2013). Indeed, tumors display a wide diversity in genomic instability, both across and within cancer types. In tumors harboring many alterations, one should not be surprised to see simultaneous alterations in any pair of genes. In contrast, two genes altered in a tumor carrying a small number of alterations might instead have resulted from a purifying selective process. Suggesting synergy as an explanation for observed co-occurrence is only reasonable if a simpler explanation like tumor-specific alteration rates can be rejected.

In this paper, we address the statistical implications of heterogeneous alteration rates across tumors for co-occurrence and mutual exclusivity detection. With extensive analyses of simulated data, we show how commonly used statistical tests are not equipped to deal with the mismatch between what is assumed by the test and what is encountered in the data. In the presence of heterogeneous alteration rates, countless spurious co-occurrences are picked up in data that are controlled not to contain any. At the same time, many instances of true mutual exclusivity are missed. Based on these observations, we introduce a novel statistical independence test that incorporates the overall alteration rates of tumors to successfully solve the issues observed before.

We applied this test to a selection of more than 3,000 tumors across 12 different cancer types. Only one co-occurrence was detected that is not explained by overall rates of alteration alone. On the other hand, many more cases of mutual exclusivity were detected than would have been possible with traditional tests. The genes targeted by these alterations cover many of the core cancer pathways known to display such exclusivity. However, we also identified exclusivity among less canonical actors in the cell cycle, and among regulators of Hedgehog signaling.

2 Results

2.1 Common tests for co-occurrence or mutual exclusivity assume homogeneous alteration rates

A commonly used test for both co-occurrence and mutual exclusivity is Fisher's exact test applied to a 2×2 contingency table (Milosevic et al. 2012; Kandoth et al. 2013; Remy et al. 2015). The test is used to support co-occurrence when the number of tumors with alterations in both genes is significantly higher than expected by chance. Likewise, it suggests mutual exclusivity when the number of tumors with alterations in both genes is significantly lower. The validity of this test depends on the assumption that genes' alterations across tumors are independent—a reasonable assumption—and identically distributed (i.i.d.). The latter implies that the probability of an alteration in a gene is the same for any given tumor. With cancer's heterogeneity in mind, this assumption may prove more problematic. Surely, a gene is more likely found altered in tumors with many somatic alterations overall, than in tumors with only few such changes.

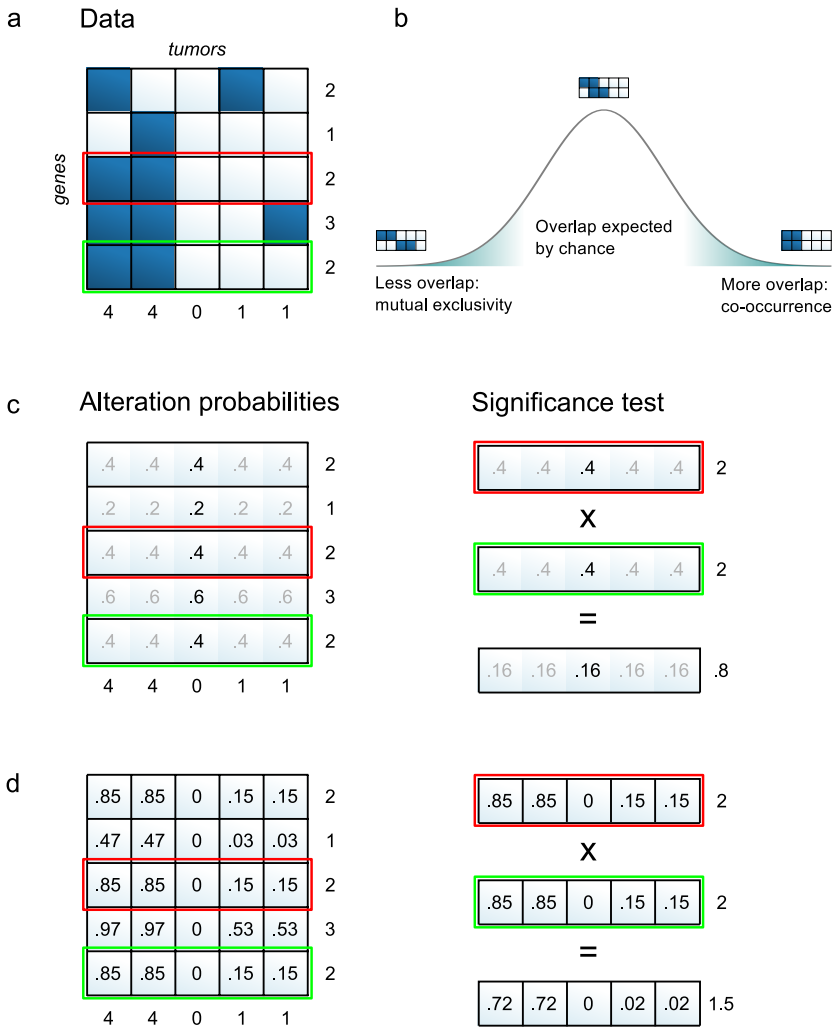

Figure 1: Overview of the DISCOVER method. (a) The input to the method is a binary alteration matrix with genes in the rows and tumors in the columns. The following panels illustrate how the two genes highlighted in red and green are tested for co-occurrence. (b) To identify co-occurrences or mutual exclusivities, a null distribution is estimated that describes the overlap in alterations of two genes expected by chance. Co-occurrence and mutual exclusivity correspond to the tails of this distribution. (c) In the Binomial model, a single alteration probability is estimated per gene that applies to all tumors. The expected number of alterations per gene matches the observed number. The expected number of alterations per tumor does not match the observed number. The product of two genes' alteration probabilities gives the probability of overlap by chance, which multiplied by the number of tumors gives

the expected number of tumors with alterations in both genes, in this case 0.8. (d) In the Poisson-Binomial model, gene alteration probabilities are estimated for each tumor individually. The expected number of alterations both per gene and per tumor match the observed numbers. The product of two gene alteration probabilities is also computed per tumor. The expected number of tumors with alterations in both genes according to this model is 1.5.

Other tests used for co-occurrence or mutual exclusivity depend on the same i.i.d. assumption as described for Fisher's exact test. This is the case for permutation tests that estimate the expected number of tumors altered in both genes by randomly reassigning gene alterations across tumors (Bredel et al. 2009; Vandin et al. 2012). It is also true for a simple Binomial test that we will use to illustrate the consequences of violating the i.i.d. assumption. This test is depicted in Figure 1c. The alteration probability p_i of a gene is estimated to be the proportion of tumors altered in that gene. For example, gene 3 in Figure 1a is altered in 2 of the 5 tumors, resulting in $p_3 = 0.4$ (Fig. 1c). If alterations targeting two genes are independent, the probability of a tumor altered in both genes equals the product $p_1 \cdot p_2$ of those genes' alteration probabilities. Hence, out of m tumors, $m \cdot p_1 p_2$ tumors are expected to harbor alterations in both genes. In the example in Figure 1a, the probability of alterations in both genes 3 and 5 would be $p_3 \cdot p_5 = 0.4 \cdot 0.4 = 0.16$. Therefore, if alterations of genes 3 and 5 were independent, we would expect $5 \cdot 0.16 = 0.8$ tumors with alterations in both. Observing more such tumors suggests co-occurrence, whereas observing fewer suggests mutual exclusivity (Fig. 1b).

2.2 Assuming homogeneous alteration rates leads to invalid significance estimates

To illustrate the effect of the i.i.d. assumption on the detection of mutual exclusivities and co-occurrences, we performed analyses on simulated data. Genomic alterations were generated such that the alteration frequencies both per gene and per tumor resemble those observed in real tumors, but without any designed relation between the genes' alterations—i.e. genes were simulated to be independent. As these simulated data do not contain co-occurrences or mutual exclusivities, all identified departures from independence are by definition spurious. We can therefore use these data to check the validity of the Binomial test. When testing many pairs of independently altered genes, a valid statistical test should produce P-values that approximately follow a uniform distribution. In contrast, when we test for co-occurrence in these data, the P-value distribution shows a large skew towards extremely low values (Fig. 2a). Even highly conservative significance levels will mark the majority of gene pairs as significant hits. Given that no true co-occurrences exist in the

simulated data, all these hits are false positives. If we test for mutual exclusivities instead, we observe a skew towards the high end of the *P*-value spectrum (Fig. 2c).

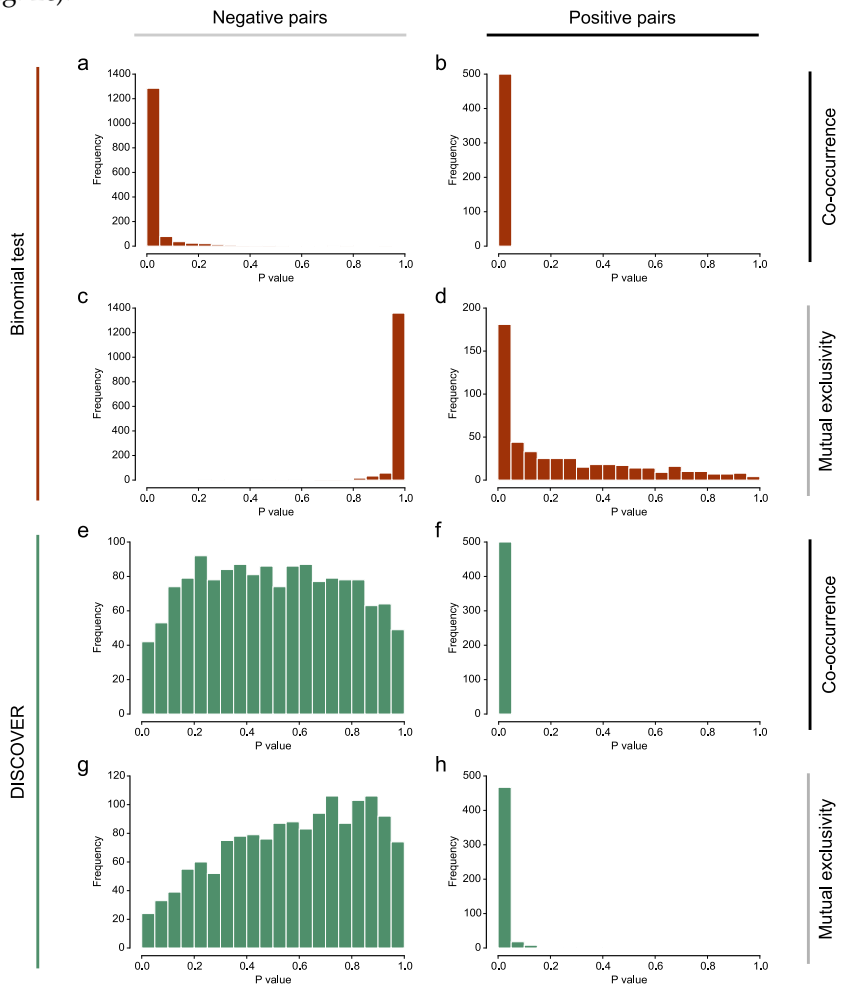

Figure 2: Histograms of *P*-values obtained on simulated data using either the Binomial test (a-d) or the DISCOVER test (e-h). The *P*-values apply to gene pairs with three different types of relation: gene pairs with independent alterations (a, c, e, g), gene pairs with co-occurring alterations (b, f), and gene pairs with mutually exclusive alterations (d, h).

We next evaluated the sensitivity of the Binomial test. For this, we tested simulated co-occurrences and mutual exclusivities, which we added to the data. A sensitive test should produce only low *P*-values for these positive cases, and so the resulting *P*-value distribution should be heavily skewed

towards zero. If we test for co-occurrences, this is indeed the case (Fig. 2b). Testing for mutual exclusivity however, reveals a distribution that, although skewed towards lower *P*-values, is much more stretched out across the [0, 1] interval (Fig. 2d). Even highly liberal significance levels will only recover a small part of the positive cases.

We conclude that the Binomial test is anti-conservative as a co-occurrence test. In contrast, as a mutual exclusivity test, it is conservative. While we used the Binomial test for this illustration, we found the same to be true for Fisher's exact test (Supplemental Fig. 1). To confirm our hypothesis that the i.i.d. assumption is causal to this incorrect behavior, we generated additional simulated data, making sure that the overall alteration rate is similar across the tumors. Using the Binomial test to detect co-occurrence and mutual exclusivity of independent genes results in *P*-value distributions that are much closer to uniform (Supplemental Fig. 2). This confirms that statistical tests that rely on the i.i.d. assumption are not suited for co-occurrence analysis, and have reduced sensitivity for mutual exclusivity analysis.

2.3 A novel statistical test for co-occurrence and mutual exclusivity

Our new method, which we call Discrete Independence Statistic Controlling for Observations with Varying Event Rates (DISCOVER), is a statistical independence test that does not assume identically distributed events. The main ingredients of the method are depicted in Figure 1d. Unlike the simpler Binomial test, we allow different tumors to have different alteration probabilities for the same gene—the alteration probabilities for genes 3 and 5 in Figure 1d now vary per tumor, in contrast to Figure 1c. For tumors with many altered genes, this probability is higher than for tumors with only few alterations. To estimate these alteration probabilities, we solve a constrained optimization problem that ensures that the probabilities are consistent with both the observed number of alterations per gene and the observed number of alterations per tumor. The probability of concurrent alterations in two independent genes is then obtained for each tumor individually, by multiplying the tumor-specific gene alteration probabilities, as indicated in the right panel of Figure 1d. With these probabilities, an analytical test based on the Poisson-Binomial distribution can be performed to decide whether the number of tumors altered in both genes deviates from the expectation.

We repeated the simulation study performed for the Binomial test, this time applying the DISCOVER test. First, our data only contained independently generated alterations. Testing for co-occurrence (Fig. 2e) and mutual exclusivity (Fig. 2g) resulted in *P*-value distributions much closer to uniform, as one would expect. The fact that these distributions are not truly uniform is a property shared by all discrete test statistics (Lancaster 1961); it makes dis-

crete tests slightly more conservative. Most importantly, the anti-conservative bias towards co-occurrence of the Binomial test is not present in the DISCOVER test. By testing simulated co-occurrences, we established that the removal of the anti-conservative bias does not compromise the sensitivity for true co-occurrences (Fig. 2f). Moreover, the sensitivity for mutual exclusivities is improved when compared with the Binomial test (Fig. 2h).

2.4 Extension to a group-based mutual exclusivity test

Mutual exclusivity is not restricted to pairs of genes. Larger groups of genes may also display alteration patterns in which most tumors only have an alteration in one of the genes. We considered three statistics to assess the mutual exclusivity of groups of genes: coverage, exclusivity, and impurity (Fig. 3a). For all three of these statistics, its expectation for groups of independent genes can be described by a Poisson-Binomial distribution (see Methods), and thus a statistical test can be formulated for determining significance. Based on simulated data, we established that the impurity-based group test has the best balance between sensitivity and specificity (Supplemental Fig. 3).

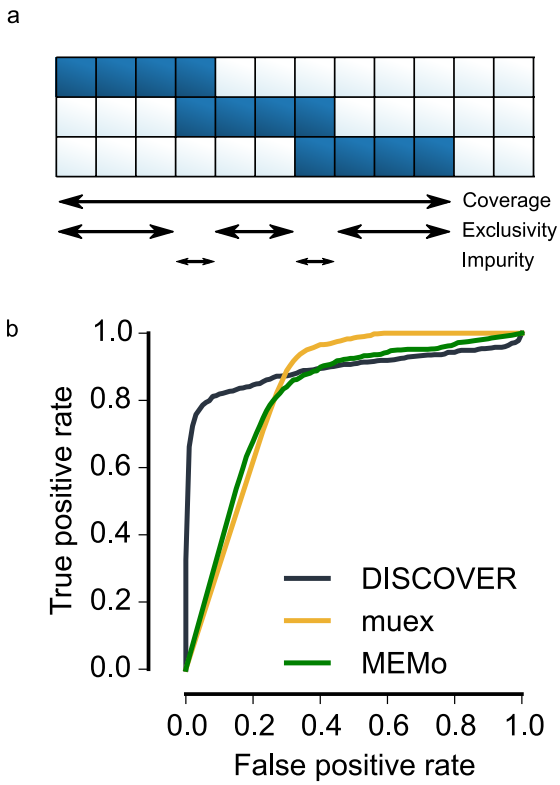

Figure 3: Extension of the DISCOVER test for mutual exclusivity within groups of genes. (a) Three alternative statistics for measuring the degree of mutual exclusivity within a group of genes. Coverage refers to the number of tumors that have an alteration in at least one of the genes. Exclusivity refers to the number of tumors that have an alteration in exactly one gene. Impurity refers to the number of tumors that have an alteration in more than one gene. (b) ROC curves comparing the performance of the DISCOVER (AUC: 0.89), muex (AUC: 0.83), and MEMo (AUC: 0.81) tests on simulated gene sets.

We compared the performance of this group-based DISCOVER test to that of two other published mutual exclusivity tests: *MEMo* (Ciriello et al. 2012) and *muex* (Szczurek and Beerenwinkel 2014). MEMo combines a permutation test for mutual exclusivity with an algorithm that identifies groups of genes to test. In our comparison, we evaluate the mutual exclusivity tests applied to pre-identified groups of genes, and thus only consider the permutation test used by MEMo, which we will refer to as the MEMo test. This test is based on the coverage statistic. Significance is assessed by a permutation method that takes into account tumor-specific alteration rates. Unlike the DISCOVER test, it estimates this alteration rate with respect to a small set of recurrently altered genes as opposed to all genes. The muex test considers both the coverage and the impurity of a group of genes. In assessing significance, identical alteration probabilities are assumed. It is thus, like Fisher's exact test, another example of a test based on the i.i.d. assumption.

The comparison was performed on simulated data. Groups of genes with mutually exclusive alterations of various degrees of impurity served as positive examples. For each such group, we also selected groups of independent genes of the same size and matched to have similar alteration frequencies, to serve as negative examples. In total, 10 data sets of 100 positive and 100 negative groups were generated. Averaged ROC curves across the 10 repetitions are displayed in Figure 3b. Only the DISCOVER test combines a high sensitivity with a high specificity. Both the MEMo test and muex are only able to identify most of the mutually exclusive groups at the cost of many spurious finds. A further inspection of the results revealed that these methods show sufficient sensitivity, but are lacking in specificity by assigning low *P*-values to many negative gene sets (Supplemental Fig. 4).

2.5 Co-occurrence and mutual exclusivity in pan-cancer somatic alterations

We analyzed a set of 3,386 tumors covering the 12 cancer types studied in the TCGA pan-cancer initiative (The Cancer Genome Atlas Research Network et al. 2013). An alteration matrix was constructed from recurrent copy number changes and high-confidence mutational drivers. Copy number changes were

analyzed for 118 genes, of which 40 gains and 78 losses. In addition, mutation data was added for 286 genes previously classified as high-confidence driver genes (Tamborero et al. 2013). In total 404 genomic alterations were analyzed covering 374 unique genes, as 30 genes are frequently targeted by both copy number changes and mutations.

We tested for pairwise co-occurrence and mutual exclusivity between pairs of genes not located on the same chromosome. These tests were stratified for cancer type to avoid confounding due to cancer type-specific alteration frequencies. Complementing the pairwise tests, we also employed the DISCOVER group test to detect patterns of mutual exclusivity in larger groups of genes. The groups we tested were selected using two different approaches. In the first approach, we extracted gene sets from the canonical pathway collection of MSigDB (Subramanian et al. 2005). We tested 23 such gene sets based on pathway membership. In the second approach, we aimed to detect de novo gene sets purely based on the data. For this, we applied a clustering algorithm to the pairwise mutual exclusivity results to identify groups of genes showing a high degree of interaction.

2.6 No evidence for widespread co-occurrence

A remarkable outcome of our analysis is that we found no evidence for widespread co-occurrence of somatic alterations. At a maximum false discovery rate (FDR) of 1%, no significant co-occurrences were identified. Relaxing the FDR threshold to 3%, we could recover one co-occurrence, between mutation of *TP53* and amplification of *MYC*. It was recently suggested that *MYC*-amplified tumors show higher levels of *MYC* expression in tumors with a *TP53* mutation than in tumors without (Ulz et al. 2016). No further, reasonable relaxation of the significance threshold led to additional hits. Certainly, more gene pairs exist that harbor alterations in overlapping sets of tumors. Yet, the sizes of those overlaps do not exceed what is expected by chance if differences in tumor-specific alteration rates are taken into account. This is in sharp contrast with the significance estimates obtained with the Binomial test, which identifies 21,627 significant co-occurrences, almost one third of all pairs tested.

With the aim of establishing that the DISCOVER test is not overly conservative, we tested for co-occurrence between copy number changes of genes on the same chromosomes. Due to the inherent correlation in copy number of genes situated close to each other, such gene pairs can be considered positive controls. Indeed, all but one of the 112 pairs of tested genes located in the same recurrently altered segment are identified as co-occurring by the DISCOVER test. In addition, 18 pairs of genes situated on the same chromosome arm are detected as co-occurring, as are *DDAH1* on 1p22 and *MCL1* on 1q21. More generally, pairs within the same segment are assigned lower *P*-values

on average than are pairs within the same chromosome arm ($P = 7 \times 10^{-39}$, Supplemental Fig. 5). The same is true, to lesser extents, for pairs within the same chromosome arm compared to pairs within the same chromosome ($P = 6 \times 10^{-8}$), and for pairs within the same chromosome compared to pairs across chromosomes ($P = 0.0004$).

2.7 Mutually exclusive alterations target core cancer pathways

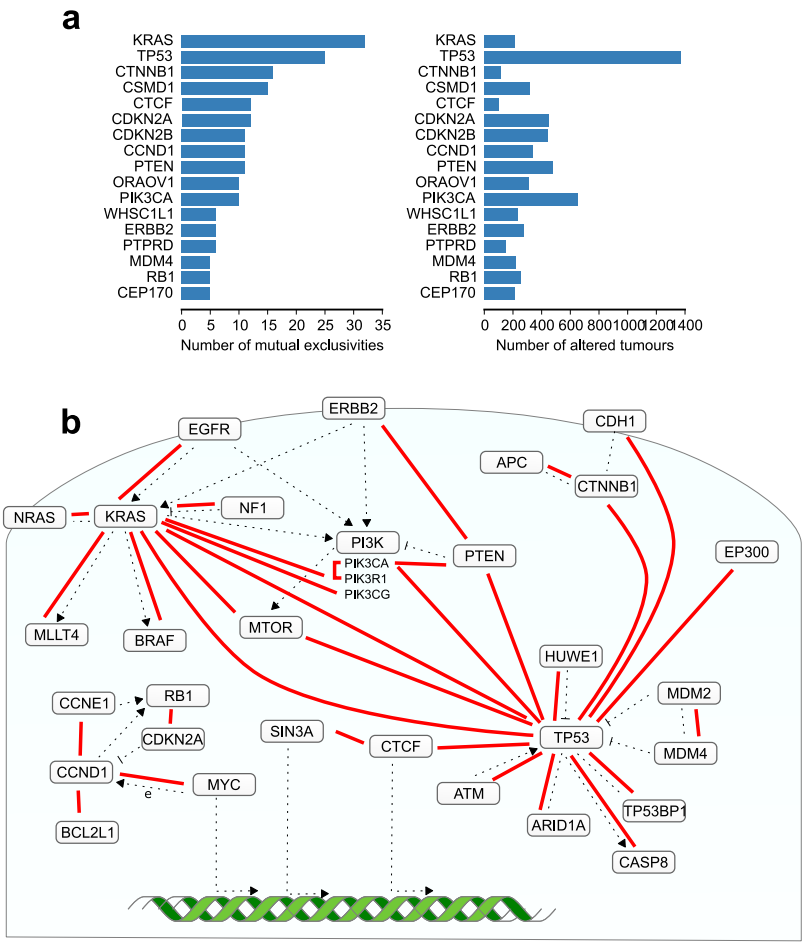

Figure 4: Overview of detected pairwise mutual exclusivities. (a) Comparison of the number of significant mutual exclusivities found for a gene and the number of tumors in which it has been altered. (b) Mutual exclusivities that overlap with high confidence interactions in the STRING functional interaction network depicted in their biological context. Red lines represent a mutual exclusivity between the connected genes. Dotted lines depict a functional in-

teraction.

Pairwise mutual exclusivities were found among 181 pairs of genes, at a maximum false discovery rate of 1% (Supplemental Table 1). We once more confirmed that detecting mutual exclusivities using the Binomial test results in far fewer significant mutual exclusivities—only three pairs were identified. Among the 181 gene pairs, there were 107 unique genes. Many of these are significantly mutually exclusive with only one or a few other genes. For some, reduced statistical power due to low alteration frequency may be the reason for not detecting more associations. However, alteration frequency is not the dominant factor in how often mutual exclusivity is detected (Fig. 4a). For example, mutations of *KRAS* are far less frequent than *TP53* or *PIK3CA* mutations. Yet, *KRAS* was found mutually exclusive with more genes than were the latter two genes.

Since mutual exclusivity is believed often to occur between functionally related genes, we determined the overlap of the identified gene pairs with the STRING functional interaction network (Szklarczyk et al. 2015). 31 of the identified gene pairs have a high-confidence functional interaction in STRING (Fig. 4b). This overlap is significantly higher than the 5 overlapping pairs expected by chance ($P < 1 \times 10^{-4}$), as determined using a permutation test. Moreover, 121 of the mutually exclusive gene pairs share a common interactor in the STRING network. By chance, this is only expected to be the case for 80 gene pairs ($P = 0.003$). This suggests that the mutual exclusivities identified are indeed for a large part driven by biological factors. The mutual exclusivities that overlap with STRING interactions revolve around three commonly deregulated processes in cancer: growth factor signaling, cell cycle control, and p53 signaling.

2.7.1 Growth factor signaling

Genes coding for proteins involved in growth factor signaling are frequently altered in cancer. These alterations display a high degree of mutual exclusivity. Mutations targeting the receptor *EGFR* are mutually exclusive with mutations in its downstream mediator *KRAS*. In turn, *KRAS* mutations are mutually exclusive with mutations in its family member *NRAS*, its negative regulator *NF1*, and its downstream effector *BRAF*. All of these alterations are able to deregulate RAS signaling, and one is sufficient. Mutual exclusivity of mutations in *KRAS* and mutations in both *PIK3R1* and *PIK3CG* may be driven by the known cross-talk between RAS signaling and PI3-kinase (PI3K) signaling (Rodriguez-Viciana et al. 1994).

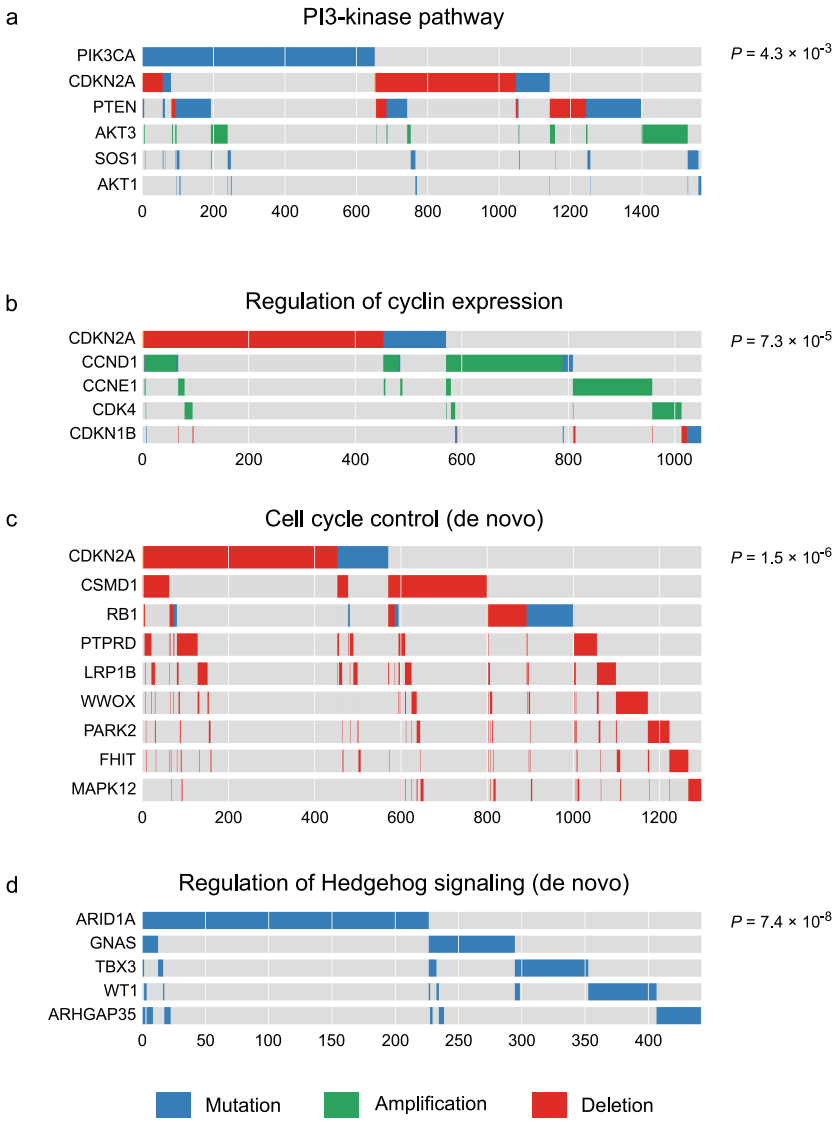

Figure 5: Examples of gene sets with mutually exclusive alterations. The *P*-values were computed using DISCOVER's group-based test. Panels a and b show predefined gene sets extracted from MSigDb. Panels c and d show gene sets identified using our de novo group detection approach.

The PI3K signaling cascade itself is also characterized by many mutually exclusive alterations. Mutations in the *PIK3CA* and *PIK3R1* genes—both coding for components of the PI3K complex—are mutually exclusive. Alterations in the *PTEN* gene—a negative regulator of the downstream activation of AKT

by PI3K—are mutually exclusive with mutations in *PIK3CA*, but also with alterations in the upstream activator of the cascade *ERBB2*. PI3K signaling is also the central biological process in several of the gene sets found mutually exclusive with the group-based test (Fig. 5a, Supplemental Fig. 6). Central genes in PI3K signaling such as *SOS1*, *AKT1*, and *AKT3* were not found as mutually exclusive with other pathway members in the pairwise analysis, yet the groupwise test correctly detects it.

2.7.2 Cell cycle control

Many tumors harbor alterations that disable the cell cycle control present in healthy cells. This control arises from a tightly regulated interplay between cell cycle activating Cyclins and CDKs, and CDK inhibitors, linked together by the master cell cycle regulator RB1. Alterations in these genes are also mutually exclusive. For example, copy number gains in *Cyclins D1* and *E1* are mutually exclusive, as are *CDKN2A* copy number loss and both mutation and copy number loss of *RB1*. The transcriptional activation of *CCND1* by *MYC* is also reflected in the mutual exclusivity between copy number gains in the two genes. Also as a group, cyclins, CDKs, and CDK inhibitors show a clear pattern of mutual exclusivity (Fig. 5b, Supplemental Fig. 6). *CDK4* and *CDKN1B*, central players in the regulation of the cell cycle, did not show up in the pairwise results, but are highly exclusive with the other genes involved.

2.7.3 p53 signaling

p53 plays a pivotal role in deciding on cell fate after cellular stresses common in cancer development. For this reason, p53 mutations are the most common alterations in cancer. Not all tumors disable p53 function genetically however. Alterations in regulators of p53 provide an alternative way to deregulate p53 function in p53-wildtype tumors, but are likely redundant in tumors that already have a dysfunctional p53 protein. Indeed, we found alterations in several regulators of p53 to be mutually exclusive with *TP53* mutation. For example, mutations in its positive regulator *ATM*, but also mutations in its negative regulator *HUWE1* are mutually exclusive with *TP53* mutations. *MDM2* and *MDM4*, highly similar negative regulators of p53, have a mutually exclusive pattern of copy number gains. Mutations in *CASP8*, a downstream mediator of p53-induced apoptosis, tend also not to overlap with *TP53* mutations.

2.8 De novo gene set detection

As a final step in our analysis, we detected de novo gene sets purely based on observed patterns of mutual exclusivity, without input based on recorded biological knowledge. To this end, we applied correlation clustering to a network

derived from pairwise mutual exclusivities (see Methods). The identified clusters were tested for groupwise mutual exclusivity with the group-based test.

One of the most significant gene sets includes *RB1* and *CDKN2A*, two pivotal players in cell cycle control (Fig. 5c). *PARK2* (Gong et al. 2014), *WWOX* (Yan et al. 2015), *FHIT* (Sard et al. 1999), *PTPRD* (D Wang et al. 2014; Solomon et al. 2008), and *MAPK12* (Zarubin and Han 2005) have also all been linked to a regulating role in various phases of the cell cycle. They have been found to do so by regulating cyclins, CDKs, or CDK inhibitors. This functional similarity may explain these genes' mutual exclusivity with *RB1* and *CDKN2A*. As of yet, *LRP1B* and *CSMD1* have not been linked to cell cycle control. Their mutual exclusivity with respect to several regulators of the cell cycle may instigate further study in this direction.

Another group of genes with a high degree of mutual exclusivity ($P = 7 \times 10^{-8}$) consists of genes that have been implicated in the regulation of Hedgehog signaling (Fig. 5d). With the exception of *ARHGAP35*, all genes in this group have experimentally been linked to a regulatory role in Hedgehog signaling. *GNAS* (Regard et al. 2013; He et al. 2014), *TBX3* (Takabatake et al. 2002), and *WT1* (Kann et al. 2015) were found to directly regulate the pathway. *ARID1A*, coding for a component of the SWI/SNF complex, is likely to play a similar role, since loss of another component of this complex, Snf5 was found to lead to activation of the Hedgehog pathway (Jagani et al. 2010). Besides these two examples, several other gene sets were identified that combine known interaction partners with interesting leads for undiscovered interactions.

3 Discussion

The recent growth in the number of large genomics data sets gives rise to a parallel increase in statistical power to detect ever more complex associations. As another consequence of larger sample sizes, however, poorly matched assumptions will have an increasing impact on the results. A central assumption behind commonly used statistical tests for co-occurrence and mutual exclusivity is that a gene's alteration probability is identical across all tumors. Using simulated data, we have shown that this assumption is not only unjustified, but that it leads to a full reversal of the associations. The Binomial test we used for illustration is but a representative of a larger class of independence tests based on the same assumption. This class includes analytical approaches such as Fisher's exact test, muex (Szczurek and Beerenwinkel 2014), and CoMEt (Leiserson et al. 2015), but also permutation tests where gene alterations are uniformly shuffled across the tumors.

We have presented a novel independence test based on assumptions that better match the reality of cancer genomics data. With this new test, we analyzed tumors across 12 different cancer types for the presence of co-occurrence

and mutual exclusivity. Only one case of co-occurrence was found, whereas numerous cases of mutual exclusivity were detected. Performing the same analysis with the Binomial test led to the detection of many co-occurrences and almost no mutual exclusivity. Many of the mutual exclusivities missed by the Binomial test can be related to central processes in cancer biology. We found strong mutual exclusivity between genes involved in growth factor signaling and cell cycle control. Also lesser known players in the regulation of cell cycle and Hedgehog signaling were identified. Based on the results of our simulation study, we are confident that the vast majority of co-occurrences detected by the Binomial test are spurious.

The absence of widespread co-occurrence contradicts what was found in previous genome-wide studies. Besides, it seems counter to our expectation of positive selection for synergy that led us to look for co-occurrence in the first place. It is true that synergy resulting from the concurrent alteration of two genes has been observed. Concurrent mutation of two genes has been reported to act on a tumor's response to chemotherapy, or more generally on patient survival (Gross et al. 2014; Malinowska-Ozdowy et al. 2015). None of these phenotypes, however, have been the subject of the selection from which the original tumor emerged. Only after selective pressure for that particular phenotype has taken place—for example by treating patients—would enrichment for such co-occurrences be detected. There is no doubt cancer-driving alterations often act in concert. Yet if statistical results are to serve as support for, or even meant to identify synergy, other possible explanations for the observed co-occurrence should be accounted for. In our pan-cancer analysis, overall alteration rates explained most if not all co-occurrence.

The need to take into account higher-level structural features of samples is not unique for co-occurrence and mutual exclusivity analysis. In testing the relationship between high-dimensional gene expression data and phenotypes of interest, latent sources of heterogeneity can have a profound effect on the results. Approaches like surrogate variable analysis (Leek and Storey 2007), have been developed to adjust analyses appropriately. Similarly, genome-wide association studies face the issue of latent population substructure. Again, if ignored, such substructure can drastically alter the findings. Linear mixed models have gained popularity as a method to prevent confounding (Yu et al. 2006). Both of these examples have become standard methodologies in many biomedical analyses. With this work, we hope to achieve that researchers performing analysis of co-occurrence and mutual exclusivity will take note of the methodological issues of commonly used tests, and we propose DISCOVER as a usable alternative.

4 Methods

4.1 Independence statistic

We assess both co-occurrence and mutual exclusivity by counting how many tumors have an alteration in both genes and comparing this to the number of tumors expected to have such an overlap by chance if these alterations were independent. Importantly, the overlap expected by chance should factor in the fact that tumors with many alterations have a higher chance of such overlap than tumors with fewer alterations. Our null distribution modeling this overlap therefore takes into account both the alteration rate per gene, and the alteration rate per tumor. To this end, let p_{ij} denote the probability of an alteration in gene i and tumor j. We assume that the alteration probability of a gene is higher in tumors with many alterations overall, than in tumors with fewer alterations. Therefore, p_{ij} may be different from p_{ik} for the same gene i in two different tumors i and k. Then, for two independent genes with alteration probabilities p_{1j} and p_{2j}, the probability of an alteration in both genes in tumor j is $p_{1j}p_{2j}$, while for tumor k it is $p_{1k}p_{2k}$. Given such probabilities for a set of tumors, the number of tumors that have an alteration in both genes follows a Poisson-Binomial distribution.

The Poisson-Binomial distribution (YH Wang 1993) describes the sum of independent, non-identically distributed Bernoulli random variables that have success probabilities $p_1, p_2, \ldots, p_n$. Its probability mass function is defined as follows.

$$\mathrm{P}(X = x) = \sum_{A \in \mathcal{F}_x} \Big(\prod_{i \in A} p_i \prod_{j \in A^c} (1 - p_j) \Big)$$

Here, $\mathcal{F}_x$ contains all subsets of size x of $\{1, 2, \ldots, n\}$, and A^c denotes the complement of A.

Based on this distribution, we can estimate the probability of observing a number of tumors with alterations in two genes as extreme—as high for co-occurrence, or as low for mutual exclusivity—as the one observed.

If, for a given gene i, all probabilities p_{ij} are equal for every tumor j, then the Poisson-Binomial distribution reduces to a Binomial distribution. However, estimating an individual alteration probability for every single tumor, ensures that the heterogeneity in alteration rates across tumors is taken into account.

4.2 Estimating gene- and tumor-specific alteration probabilities

To apply the DISCOVER test, we need estimates of the alteration probabilities p_{ij} for all genes i and all tumors j. Let $\mathcal{X} \in \{0, 1\}^{n \times m}$ denote the $n \times m$ binary alteration matrix where an entry x_{ij} is 1 in case of an alteration in gene i and

tumor j, and 0 otherwise. We use the notation $x_{i\bullet}$ and $x_{\bullet j}$ for the marginal sums of the ith row and jth column respectively. Furthermore, let X_{ij} denote the random variable for x_{ij}, and $X_{i\bullet}$ and $X_{\bullet j}$ the corresponding marginal sums. If we were to assume that the alteration of a gene is equally likely across all tumors, then the alteration probability only depends on the number of altered tumors $x_{i\bullet}$ and the total number of tumors m.

$$p_{ij} = \mathrm{P}(X_{ij} = 1 | x_{i\bullet} = k) = \frac{k}{m}, \forall j$$

Estimating the alteration probabilities this way ensures that the expected number of alterations $\mathrm{E}_p(X_{i\bullet}) = \sum_j p_{ij}$ for a gene matches the observed number $x_{i\bullet}$. In fact, the familiar expression above, is the one that maximizes the likelihood of the observed alterations under the constraint that the expected number of alterations per gene matches the observed number. To make this more explicit, we can reformulate the probability estimation as a constrained optimization problem.

$$\begin{aligned}
\max_p \quad & \mathrm{L}_p(\mathcal{X}) = \sum_{i=1}^{n}\sum_{j=1}^{m} p_{ij}x_{ij} + (1-p_{ij})(1-x_{ij}) \\
\text{s.t.} \quad & \\
& \sum_{j=1}^{m} p_{ij} = \sum_{j=1}^{m} x_{ij} && , \quad 1 \le i \le n \\
& 0 \le p_{ij} \le 1 && , \quad 1 \le i \le n, 1 \le j \le m
\end{aligned}$$

All of the above is based on the assumption that alteration probabilities for a gene are equal across tumors. Symptomatic for this assumption are probability estimates such that the expected number of alterations per tumor $\mathrm{E}_p(X_{\bullet j}) = \sum_i p_{ij}$ generally does not match the observed number $x_{\bullet j}$. To take into account tumor-specific alteration rates, the above optimization problem can be extended such that this expectation is also matched.

$$\begin{aligned}
\max_p \quad & \mathrm{H}_p(\mathcal{X}) = -\sum_{i=1}^{n}\sum_{j=1}^{m} p_{ij}\log(p_{ij}) + (1-p_{ij})\log(1-p_{ij}) \\
\text{s.t.} \quad & \\
& \sum_{c=1}^{m} p_{ic} = \sum_{c=1}^{m} x_{ic} && , \quad 1 \le i \le n \\
& \sum_{r=1}^{n} p_{rj} = \sum_{r=1}^{n} x_{rj} && , \quad 1 \le j \le m \\
& 0 \le p_{ij} \le 1 && , \quad 1 \le i \le n, 1 \le j \le m
\end{aligned}$$

With this new formulation, the number of parameters to fit is increased by a factor m. As a consequence, optimizing the likelihood $\mathrm{L}_p(\mathcal{X})$ of the model risks overfitting the data. Therefore, instead of optimizing the likelihood we choose to optimize the information entropy $\mathrm{H}_p(\mathcal{X})$. It can be shown that in the optimal solution to this reformulated problem, each alteration probability can be written in terms of two parameters (Supplemental Methods).

$$p_{ij} = \frac{1}{1 + e^{\mu_i + \lambda_j}}$$

Here, each parameter μ_i for gene i is shared by all tumors, and each parameter λ_j for tumor j is shared by all genes. Because of this, while the original optimization problem aims to estimate $n \times m$ alteration probabilities, we can obtain the optimal solution by estimating only $n + m$ parameters. Moreover, all genes with the same number of altered tumors share the same value for μ_i. Likewise, all tumors with the same number of altered genes share the same value for λ_j. This sharing of parameters leads to an even larger reduction in the effective dimensionality of the optimization.

Unlike for the Binomial case, there is no closed-form solution for estimating the μ_i and λ_j parameters. Instead, we use the quasi-Newton numerical optimization algorithm L-BFGS (Liu and Nocedal 1989).

4.3 Stratified analysis

When the data consist of clearly separate groups of tumors, such as is the case in the pan-cancer analyses with its different cancer types, it is preferable to stratify the analysis on these groups. If for example in the mutual exclusivity analysis, group structure is not taken into account, the detected mutual exclusivities may be little more than markers for the underlying cancer types, rather than biologically related genes. The DISCOVER test is easily stratified for different groups by solving the constrained optimization problem separately for the tumors of each group. The group-specific background matrices can then be concatenated to construct a single global, but stratified, parameter matrix.

4.4 False discovery rate control

Commonly used procedures for multiple testing correction assume that the *P*-values are distributed uniformly under the null hypothesis. This is the case for e.g. Bonferroni correction and the Benjamini-Hochberg procedure. However, hypothesis tests that are based on a discrete test statistic, such as our DISCOVER test, are known to lead to non-uniform *P*-value distributions under the null hypothesis. In fact, pooling the *P*-values across tests with a large set of different parameters results in a *P*-value distribution that is skewed towards 1.0. This complicates the application of the standard procedures for

multiple testing correction. While these procedures would still control the family-wise error rate or false discovery rate at the specified threshold, they will be more conservative because of the non-uniformity caused by the discrete test statistic. For the analyses in this paper, we used an adaptation of the Benjamini-Hochberg procedure for discrete test statistics (Carlson et al. 2009).

4.5 Group-based mutual exclusivity test

We have defined a family of group-based mutual exclusivity tests. The following statistics can be used to assess groupwise mutual exclusivity. Each of these statistics can be shown to follow a Poisson-Binomial distribution, which we make use of to estimate significance.

- *Coverage*: the number of tumors that have an alterations in at least one of the genes. Significance is based on the probability of observing a coverage at least as high in independent genes. The Poisson-Binomial parameters for a group of genes $\{g_i \mid i \in I\}$ can be derived from the individual gene alteration probabilities as follows.

$$p_j = 1 - \prod_{i \in I} (1 - p_{ij}) \quad , \quad 1 \leq j \leq m$$

  That is, the probably of at least one alteration is one minus the probability of not having any alteration.

- *Exclusivity*: the number of tumors that have an alteration in exactly one of the genes. Significance is based on the probability of observing exclusivity at least as high in independent genes. The Poisson-Binomial parameters can be derived from the gene alteration probabilities as follows.

$$p_j = \sum_{i \in I} p_{ij} \prod_{k \in I \setminus \{i\}} (1 - p_{kj}) \quad , \quad 1 \leq j \leq m$$

- *Impurity*: the number of tumors that have an alteration in more than one gene. Significance is based on the probability of observing impurity at least as low in independent genes. The Poisson-Binomial parameters can be derived from the gene alteration probabilities as follows.

$$p_j = 1 - \prod_{i \in I} (1 - p_{ij}) - \sum_{i \in I} p_{ij} \prod_{k \in I \setminus \{i\}} (1 - p_{kj}) \quad , \quad 1 \leq j \leq m$$

  That is, the probability of more than one alteration is one minus the probabilities of no alterations and exactly one alteration. As a special

case of this, if a group of only two genes is tested, the above expression reduces to $p_j = p_{1j}p_{2j}$. This is the same parameterization as was used for the pairwise test.

4.6 Simulation data

An alteration matrix was constructed such that alteration frequencies across both genes and tumors resembled those of real tumors. For this, we used the copy number data of the TCGA breast cancer study as a reference. Based on the copy number matrix for 24,174 genes and 1,044 tumors, we constructed two sequences of marginal counts corresponding to the number of amplifications across genes and across tumors. These two sequences were used as degree sequences to construct a random bipartite graph following the configuration model. The adjacency matrix of this bipartite graph was then used as alteration matrix for the simulated data analyses. Because of the way this matrix was constructed, the alteration frequencies across both genes and tumors resemble those of the breast cancer tumors used for reference, yet there is no dependence between alterations across genes. For the analyses, only genes with at least 50 alterations were tested.

Mutually exclusive and co-occurring gene pairs, as well as mutually exclusive gene sets were generated based on two parameters: coverage, the number of tumors altered in at least one of the genes; and impurity or overlap, the proportion of covered tumors altered in more than one of the genes. To generate pairs of mutually exclusive genes, we used quantile regression to relate the coverage of independent gene pairs to their to impurity. Simulated mutually exclusive gene pairs were generated such that their impurity was below the first percentile predicted by the quantile regression model based on their coverage. Likewise, pairs of co-occurring genes were generated such that the number of tumors altered in both genes exceeded the 99th percentile based on the coverage of independent gene pairs. Mutually exclusive gene sets were generated by randomly sampling the gene set size from $\{3, 4, 5, 6\}$, the percentage of covered tumors from $\{0.2, 0.4, 0.6, 0.8\}$, and the impurity from $\{0.02, 0.05, 0.08\}$. Impure alterations, i.e. additional alterations in an already covered tumor, were assigned to tumors with a probability proportional to the tumor's overall alteration frequency.

For all analyses, the background matrix for the DISCOVER test was estimated on the complete alteration matrix, including genes with fewer than 50 alterations, and including simulated co-occurrences or mutual exclusivities.

4.7 Pan-cancer alteration data

Preprocessed somatic mutation and copy number data for the 12 cancer types studied in the TCGA pan-cancer initiative (The Cancer Genome Atlas Research Network et al. 2013) were obtained via Firehose (analysis run

2014_07_15). Mutations were extracted from the input of the MutSig 2CV analysis. Mutations for genes that have previously been identified as high-confidence mutational drivers (Tamborero et al. 2013) were included in the analysis. Discretized copy number changes were extracted from the output of GISTIC2. We considered genes altered if GISTIC2 qualified their copy number change as high-level. Pan-cancer recurrently altered regions were obtained via Synapse (syn2203662). For each region, we selected their most likely driver genes for inclusion in the analysis. If a region contained only one gene, this gene was assumed its driver. In the case of more genes, genes were selected if they overlapped with the list of high-confidence mutational driver genes, or with a curated list of cancer genes (`http://www.bushmanlab.org/links/genelists`).

Background matrices for the DISCOVER test were estimated for each type of alteration—mutation, amplification, and deletion—separately, and based on the genome-wide alteration matrices before gene selection. Stratification for the 12 different cancer types was applied as described before. The background matrix used in the analysis was subsequently composed out of the relevant rows in the three alteration type-specific background matrices.

4.8 Overlap with the STRING functional interaction network

Version 10.0 of the STRING network (Szklarczyk et al. 2015) was used to determine overlap of detected mutual exclusivities and functional interactions. We constructed a functional interaction graph by connecting genes with an edge if they have a high-confidence STRING interaction, defined by a combined score greater than 800. A mutual exclusivity graph was constructed by connecting genes with an edge if alterations in these genes were found mutually exclusive at a maximum FDR of 1%. The overlap corresponds to the number of edges appearing in both graphs. To determine enrichment of this overlap, we estimated a null distribution by randomly shuffling the gene labels of the mutual exclusivity graph 10,000 times and computing the overlap of these shuffled mutual exclusivity graphs with the unshuffled functional interaction graph.

4.9 De novo gene set detection

Our algorithm for detecting de novo sets of mutually exclusive genes combines two ideas from community detection. Its goal is to detect gene sets with a high likelihood of being mutually exclusive based on the results of a pairwise mutual exclusivity analysis. There are three main steps. First, a mutual exclusivity graph is constructed where genes are connected by an edge if their alterations have been identified as mutually exclusive by the pairwise test. For this step, we used a permissive significance criterion—a maximum FDR of 10%—so as not to exclude potentially interesting gene pairs that may

simply not have reached significance due to the limited sample size. Second, groups of genes with a high density of mutual exclusivity edges between them are identified using a graph partitioning algorithm. Finally, these groups are subjected to the groupwise mutual exclusivity test to retain only those groups that are mutually exclusive as a group.

The graph partitioning step is based on overlapping correlation clustering. In correlation clustering, nodes in a graph are clustered such that the combined weight of edges within clusters is maximized, and the combined weight of edges between clusters is minimized. The particular algorithm we used (Bonchi et al. 2013) allows nodes to be assigned to multiple clusters. Moreover, we modified the original algorithm such that groups of nodes can be designated that should always share the same cluster assignments. We used this for two situations. First, genes in the same copy number segment have highly correlated copy number alterations, and consequently highly similar mutual exclusivities. Purely based on genomic data there is no reason to prefer one gene over the other, which is why we always assign all such genes to the same cluster. Second, we assume copy number alterations and mutations targeting the same gene serve the same function, and therefore add the constraint that these are always assigned to the same cluster.

The edge weights of the mutual exclusivity graph play an important role in the objective function of correlation clustering. A common phenomenon in pairwise associations is that one gene is found mutually exclusive with many other genes, but those genes are not all mutually exclusive with each other. The edges connecting the former gene may therefore not be indicative of gene set membership. They should be assigned a lower weight than edges that more specifically connect genes with a high degree of internal connectivity. To this aim, we selected the edge weights to optimize a modularity objective. In modularity optimization, a graph is compared with random graphs having the same number of nodes, edges, and degree distribution. Edges that are specific to the graph being partitioned are preferably kept within clusters, whereas edges that also appear in many of the random graphs will often span two clusters. We used a modularity measure based on conditional expected models (Chang et al. 2012). This measure ensures that edges connecting sets of nodes with high node degrees receive a lower weight than edges that connect sets of nodes with low node degrees. In addition, it also allows for the covariance between the mutual exclusivity tests to be taken into account.

References

Ashworth A, Lord CJ, and Reis-Filho JS. 2011. Genetic interactions in cancer progression and treatment. *Cell* **145**:30–8.

Bonchi F, Gionis A, and Ukkonen A. 2013. Overlapping correlation clustering. *Knowledge and information systems* **35**:1–32.

Bredel M, Scholtens DM, Harsh GR, Bredel C, Chandler JP, Renfrow JJ, Yadav AK, Vogel H, Scheck AC, Tibshirani R, et al. 2009. A network model of a cooperative genetic landscape in brain tumors. *JAMA* **302**:261–75.

Carlson JM, Heckerman D, and Shani G. 2009. *Estimating false discovery rates for contingency tables*. Tech. rep. MSR-TR-2009-53.

Chang YT, Leahy RM, and Pantazis D. 2012. Modularity-based graph partitioning using conditional expected models. *Physical Review E* **85**:016109.

Ciriello G, Cerami E, Sander C, and Schultz N. 2012. Mutual exclusivity analysis identifies oncogenic network modules. *Genome Res* **22**:398–406.

Gong Y, Zack TI, Morris LG, Lin K, Hukkelhoven E, Raheja R, Tan IL, Turcan S, Veeriah S, Meng S, et al. 2014. Pan-cancer genetic analysis identifies PARK2 as a master regulator of G1/S cyclins. *Nat Genet* **46**:588–94.

Gorringe KL, George J, Anglesio MS, Ramakrishna M, Etemadmoghadam D, Cowin P, Sridhar A, Williams LH, Boyle SE, Yanaihara N, et al. 2010. Copy number analysis identifies novel interactions between genomic loci in ovarian cancer. *PLoS One* **5**.

Gross AM, Orosco RK, Shen JP, Egloff AM, Carter H, Hofree M, Choueiri M, Coffey CS, Lippman SM, Hayes DN, et al. 2014. Multi-tiered genomic analysis of head and neck cancer ties TP53 mutation to 3p loss. *Nat Genet* **46**:939–43.

He X, Zhang L, Chen Y, Remke M, Shih D, Lu F, Wang H, Deng Y, Yu Y, Xia Y, et al. 2014. The G protein α subunit Gαs is a tumor suppressor in Sonic hedgehog-driven medulloblastoma. *Nat Med* **20**:1035–42.

Jagani Z, Mora-Blanco EL, Sansam CG, McKenna ES, Wilson B, Chen D, Klekota J, Tamayo P, Nguyen PT, Tolstorukov M, et al. 2010. Loss of the tumor suppressor Snf5 leads to aberrant activation of the Hedgehog-Gli pathway. *Nat Med* **16**:1429–33.

Kandoth C, McLellan MD, Vandin F, Ye K, Niu B, Lu C, Xie M, Zhang Q, McMichael JF, Wyczalkowski MA, et al. 2013. Mutational landscape and significance across 12 major cancer types. *Nature* **502**:333–9.

Kann M, Bae E, Lenz MO, Li L, Trannguyen B, Schumacher VA, Taglienti ME, Bordeianou L, Hartwig S, Rinschen MM, et al. 2015. WT1 targets Gas1 to maintain nephron progenitor cells by modulating FGF signals. *Development* **142**:1254–66.

Klijn C, Bot J, Adams DJ, Reinders M, Wessels L, and Jonkers J. 2010. Identification of networks of co-occurring, tumor-related DNA copy number changes using a genome-wide scoring approach. *PLoS Comput Biol* **6**:e1000631.

Lancaster HO. 1961. Significance Tests in Discrete Distributions. *Journal of the American Statistical Association* **56**:223–234. ISSN: 01621459.

Lawrence MS, Stojanov P, Mermel CH, Robinson JT, Garraway LA, Golub TR, Meyerson M, Gabriel SB, Lander ES, and Getz G. 2014. Discovery and

saturation analysis of cancer genes across 21 tumour types. *Nature* **505**:495–501.

Leek JT and Storey JD. 2007. Capturing Heterogeneity in Gene Expression Studies by Surrogate Variable Analysis. *PLoS Genetics* **3**:e161.

Leiserson MD, Wu HT, Vandin F, and Raphael BJ. 2015. CoMEt: a statistical approach to identify combinations of mutually exclusive alterations in cancer. *Genome Biol* **16**:160.

Liu DC and Nocedal J. 1989. On the limited memory BFGS method for large scale optimization. *Mathematical programming* **45**:503–528.

Malinowska-Ozdowy K, Frech C, Schönegger A, Eckert C, Cazzaniga G, Stanulla M, Stadt U zur, Mecklenbräuker A, Schuster M, Kneidinger D, et al. 2015. KRAS and CREBBP mutations: a relapse-linked malicious liaison in childhood high hyperdiploid acute lymphoblastic leukemia. *Leukemia* **29**:1656–67.

Milosevic JD, Puda A, Malcovati L, Berg T, Hofbauer M, Stukalov A, Klampfl T, Harutyunyan AS, Gisslinger H, Gisslinger B, et al. 2012. Clinical significance of genetic aberrations in secondary acute myeloid leukemia. *Am J Hematol* **87**:1010–6.

Regard JB, Malhotra D, Gvozdenovic-Jeremic J, Josey M, Chen M, Weinstein LS, Lu J, Shore EM, Kaplan FS, and Yang Y. 2013. Activation of Hedgehog signaling by loss of GNAS causes heterotopic ossification. *Nat Med* **19**:1505–12.

Remy E, Rebouissou S, Chaouiya C, Zinovyev A, Radvanyi F, and Calzone L. 2015. A Modeling Approach to Explain Mutually Exclusive and Co-Occurring Genetic Alterations in Bladder Tumorigenesis. *Cancer Res* **75**:4042–52.

Rodriguez-Viciana P, Warne PH, Dhand R, Vanhaesebroeck B, Gout I, Fry MJ, Waterfield MD, and Downward J. 1994. Phosphatidylinositol-3-OH kinase as a direct target of Ras. *Nature* **370**:527–32.

Sard L, Accornero P, Tornielli S, Delia D, Bunone G, Campiglio M, Colombo MP, Gramegna M, Croce CM, Pierotti MA, et al. 1999. The tumor-suppressor gene FHIT is involved in the regulation of apoptosis and in cell cycle control. *Proc Natl Acad Sci U S A* **96**:8489–92.

Solomon DA, Kim JS, Cronin JC, Sibenaller Z, Ryken T, Rosenberg SA, Ressom H, Jean W, Bigner D, Yan H, et al. 2008. Mutational inactivation of PTPRD in glioblastoma multiforme and malignant melanoma. *Cancer Res* **68**:10300–6.

Subramanian A, Tamayo P, Mootha VK, Mukherjee S, Ebert BL, Gillette MA, Paulovich A, Pomeroy SL, Golub TR, Lander ES, et al. 2005. Gene set enrichment analysis: a knowledge-based approach for interpreting genome-wide expression profiles. *Proc Natl Acad Sci U S A* **102**:15545–50.

Szczurek E and Beerenwinkel N. 2014. Modeling mutual exclusivity of cancer mutations. *PLoS Comput Biol* **10**:e1003503.

Szklarczyk D, Franceschini A, Wyder S, Forslund K, Heller D, Huerta-Cepas J, Simonovic M, Roth A, Santos A, Tsafou KP, et al. 2015. STRING v10: protein-protein interaction networks, integrated over the tree of life. *Nucleic Acids Res* **43**:D447–52.

Takabatake Y, Takabatake T, Sasagawa S, and Takeshima K. 2002. Conserved expression control and shared activity between cognate T-box genes Tbx2 and Tbx3 in connection with Sonic hedgehog signaling during Xenopus eye development. *Dev Growth Differ* **44**:257–71.

Tamborero D, Gonzalez-Perez A, Perez-Llamas C, Deu-Pons J, Kandoth C, Reimand J, Lawrence MS, Getz G, Bader GD, Ding L, et al. 2013. Comprehensive identification of mutational cancer driver genes across 12 tumor types. *Sci Rep* **3**:2650.

The Cancer Genome Atlas Research Network, Weinstein JN, Collisson EA, Mills GB, Shaw KR, Ozenberger BA, Ellrott K, Shmulevich I, Sander C, and Stuart JM. 2013. The Cancer Genome Atlas Pan-Cancer analysis project. *Nat Genet* **45**:1113–20.

Thomas RK, Baker AC, Debiasi RM, Winckler W, Laframboise T, Lin WM, Wang M, Feng W, Zander T, MacConaill L, et al. 2007. High-throughput oncogene mutation profiling in human cancer. *Nat Genet* **39**:347–51.

Ulz P, Heitzer E, and Speicher MR. 2016. Co-occurrence of MYC amplification and TP53 mutations in human cancer. *Nat Genet* **48**:104–6.

Vandin F, Upfal E, and Raphael BJ. 2012. De novo discovery of mutated driver pathways in cancer. *Genome Res* **22**:375–85.

Vogelstein B, Papadopoulos N, Velculescu VE, Zhou S, Diaz Jr LA, and Kinzler KW. 2013. Cancer genome landscapes. *Science* **339**:1546–58.

Wang D, Wang L, Zhou J, Pan J, Qian W, Fu J, Zhang G, Zhu Y, Liu C, Wang C, et al. 2014. Reduced expression of PTPRD correlates with poor prognosis in gastric adenocarcinoma. *PLoS One* **9**:e113754.

Wang YH. 1993. On the number of successes in independent trials. *Statistica Sinica* **3**:295–312.

Yan H, Tong J, Lin X, Han Q, and Huang H. 2015. Effect of the WWOX gene on the regulation of the cell cycle and apoptosis in human ovarian cancer stem cells. *Mol Med Rep* **12**:1783–8.

Yeang CH, McCormick F, and Levine A. 2008. Combinatorial patterns of somatic gene mutations in cancer. *FASEB J* **22**:2605–22.

Yu J, Pressoir G, Briggs WH, Vroh Bi I, Yamasaki M, Doebley JF, McMullen MD, Gaut BS, Nielsen DM, Holland JB, et al. 2006. A unified mixed-model method for association mapping that accounts for multiple levels of relatedness. *Nat Genet* **38**:203–8.

Zack TI, Schumacher SE, Carter SL, Cherniack AD, Saksena G, Tabak B, Lawrence MS, Zhang CZ, Wala J, Mermel CH, et al. 2013. Pan-cancer patterns of somatic copy number alteration. *Nature genetics* **45**:1134–1140. ISSN: 1546-1718.

Zarubin T and Han J. 2005. Activation and signaling of the p38 MAP kinase pathway. *Cell Res* **15**:11–8.

Supplemental figures

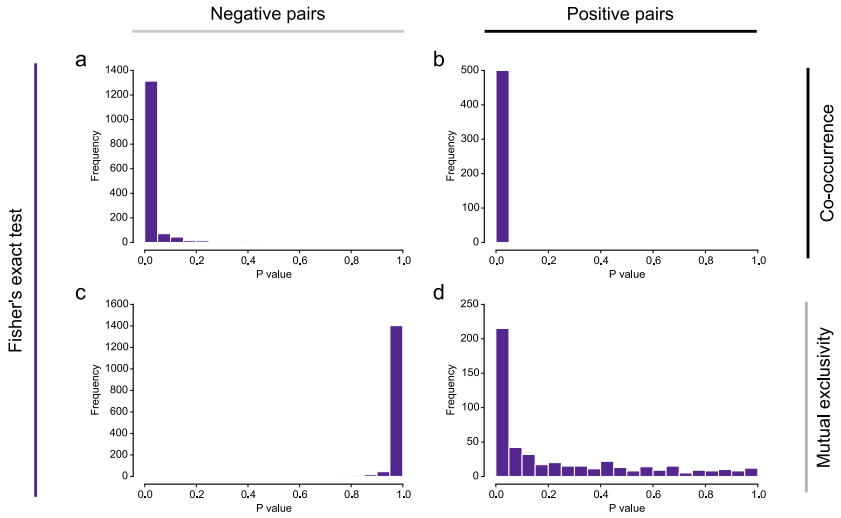

Supplemental Figure 1: Histograms of *P*-values obtained on simulated data using Fisher's exact test. The *P*-values apply to gene pairs with three different types of relation: gene pairs with independent alterations (a, c), gene pairs with co-occurring alterations (b), and gene pairs with mutually exclusive alterations (d).

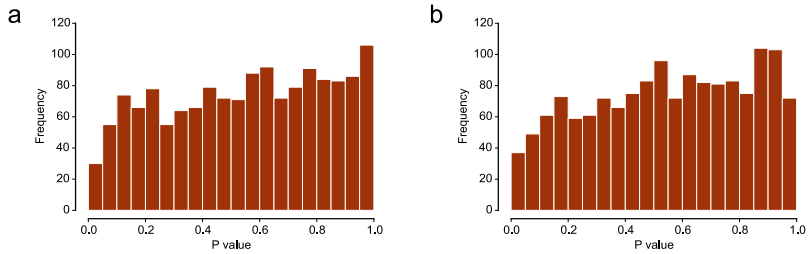

Supplemental Figure 2: Histograms of *P*-values obtained by testing independent gene pairs for either co-occurrence (a) or mutual exclusivity (b) using the Binomial test. Simulated alteration data were generated in such a way that gene alteration frequencies resemble those in real tumors. Alteration frequencies of tumors are similar for all tumors.

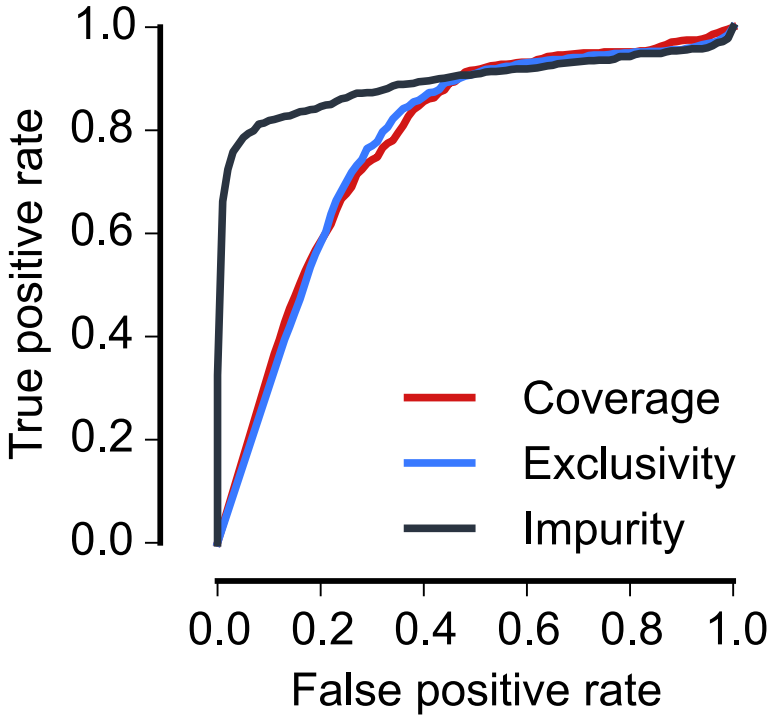

Supplemental Figure 3: ROC curves describing the performance on simulated gene sets of the DISCOVER test based on three alternative statistics: Coverage, the number of tumors that have an alteration in at least one of the genes; Exclusivity, the number of tumors that have an alteration in exactly one gene; Impurity, the number of tumors that have an alteration in more than one gene.

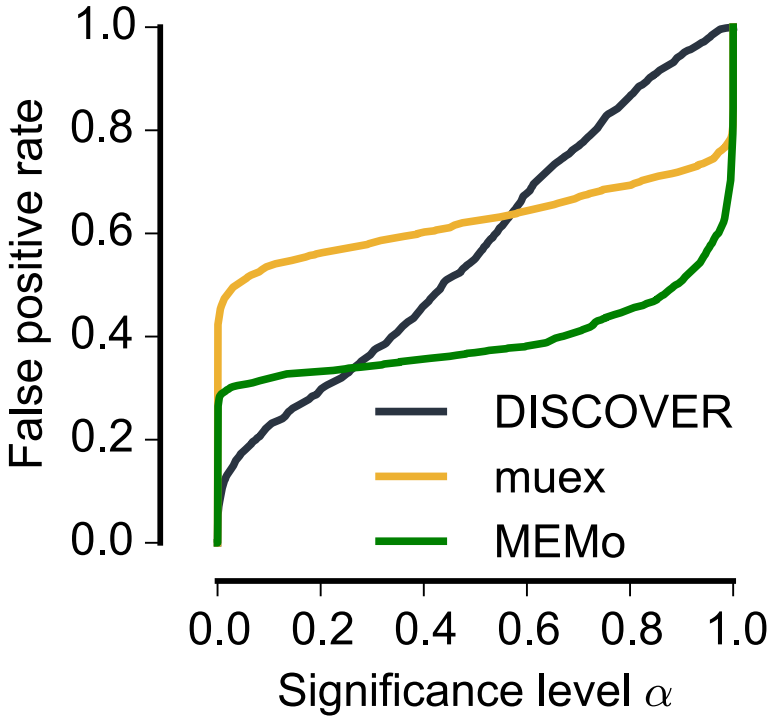

Supplemental Figure 4: *P*-value calibration curves for the DISCOVER, muex, and MEMo group tests. For a statistical test, the significance level α should approximate the false positive rate. In such a case, the calibration curve would be a diagonal line. For the DISCOVER test, the calibration curve is close to diagonal. For the MEMo test, significance levels up to approximately 0.3 lead to higher false positive rates, while for higher significance levels the false positive rate is overestimated. This is even more extreme for muex.

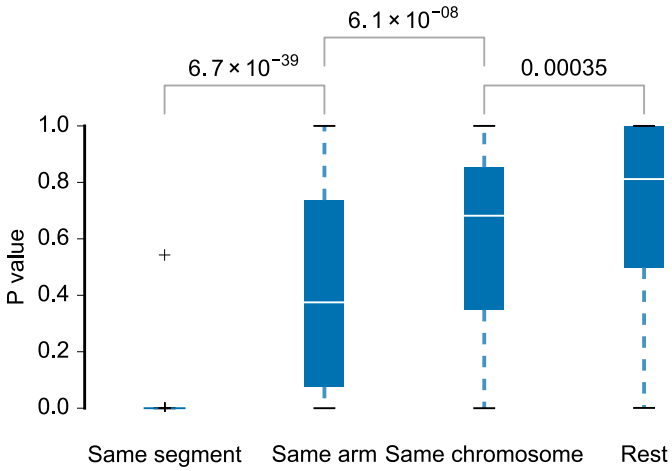

Supplemental Figure 5: Comparison of *P*-values obtained when testing for co-occurrence between genes within the same recurrently altered segment, within the same chromosome arm, within the same chromosome, and across chromosomes. Differences in mean are tested with the Mann-Whitney *U* test.

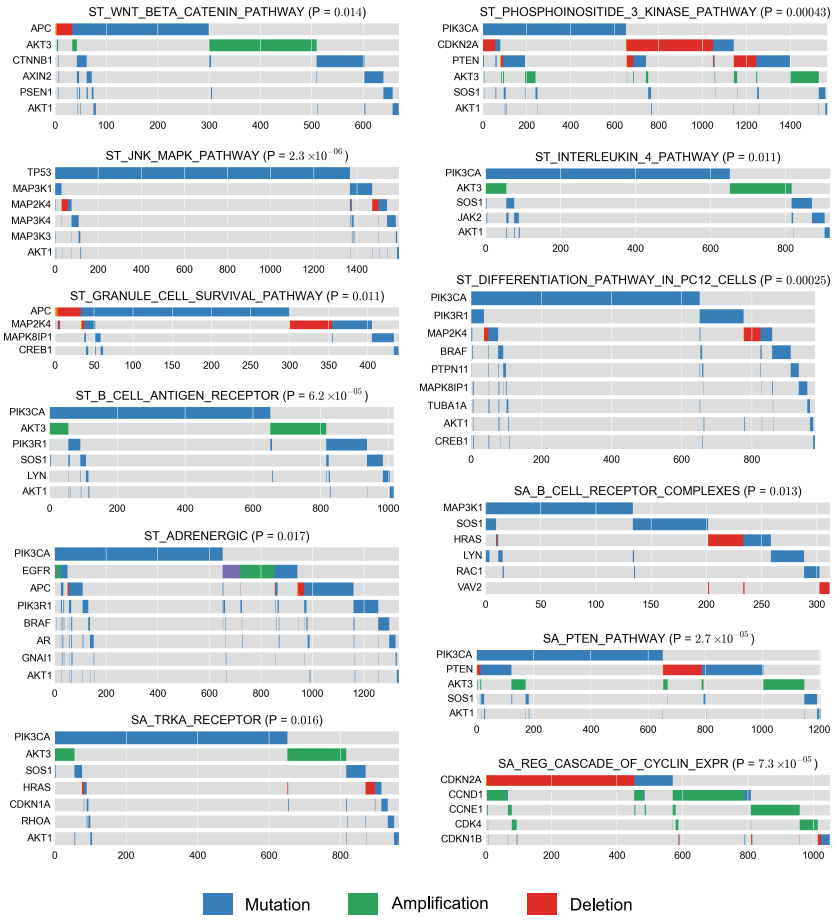

Supplemental Figure 6: Overview of the significantly mutually exclusive gene sets from the MSigDb canonical pathway collection.

Supplemental tables

Supplemental Table 1: Significantly mutually exclusive alterations found in the pan-cancer data at a maximum FDR of 1%. The first four columns show the genes and the types of alteration involved (mut = point mutation; gain, loss = copy number gain, loss). The *P*-value is obtained using DISCOVER's mutual exclusivity test. The *Q*-value is the false discover rate estimated using the method of Carlson et al.(Carlson et al. 2009)

Gene 1	Gene 1 alteration	Gene 2	Gene 2 alteration	*P*-value	*Q*-value
CDH1	mut	TP53	mut	6.7e-15	4.6e-12
PIK3CA	mut	PIK3R1	mut	4.1e-14	1.6e-11
CSMD1	loss	CDKN2A	loss	2.9e-13	8.2e-11
PTEN	loss	CSMD1	loss	3.4e-13	8.2e-11
CSMD1	loss	CDKN2B	loss	1e-12	2.2e-10
TP53	mut	PIK3CA	mut	1.6e-12	2.9e-10
ARID1A	mut	TP53	mut	2.7e-12	4e-10
TP53	mut	CTNNB1	mut	2.7e-12	4e-10
TP53	mut	MAP3K1	mut	4.2e-11	7e-09
KRAS	mut	TP53	mut	1.2e-10	2e-08
ATM	mut	TP53	mut	1.6e-10	2.4e-08
FHIT	loss	CSMD1	loss	3.2e-10	4.9e-08
CTCF	mut	TP53	mut	1.8e-09	3e-07
GATA3	mut	TP53	mut	4e-09	7.1e-07
RB1	loss	CDKN2A	loss	5.5e-09	9.5e-07
KRAS	mut	CTNNB1	mut	7.6e-09	1.2e-06
PTEN	mut	TP53	mut	7.8e-09	1.2e-06
RB1	loss	CDKN2B	loss	8.2e-09	1.2e-06
KRAS	mut	SPOP	mut	1e-08	1.5e-06
KRAS	mut	BRAF	mut	1.2e-08	1.7e-06
RB1	loss	CSMD1	loss	2.4e-08	3.5e-06
RB1	loss	PTPRD	loss	6.1e-08	9.5e-06
KRAS	mut	CTCF	mut	8.7e-08	1.4e-05
FGFR2	mut	KRAS	mut	1.2e-07	1.8e-05
PTEN	loss	PTPRD	loss	2.3e-07	3.8e-05
PPP2R1A	mut	PIK3R1	mut	4e-07	6.6e-05
TP53	mut	PIK3R1	mut	4.3e-07	6.8e-05
CEP170	gain	WHSC1L1	gain	4.4e-07	6.8e-05
PTEN	loss	CDKN2B	loss	5.2e-07	7.9e-05
CTNNB1	mut	FBXW7	mut	6.2e-07	9.4e-05
LRP1B	loss	CDKN2B	loss	6.7e-07	9.8e-05
ZFHX3	mut	TP53	mut	8.1e-07	0.00012

PTEN	loss	CDKN2A	loss	8.4e-07	0.00012
NFATC1	loss	CSMD1	loss	8.4e-07	0.00012
WWOX	loss	CSMD1	loss	1.1e-06	0.00015
MLL2	mut	CTCF	mut	1.1e-06	0.00015
ZFHX3	mut	CTNNB1	mut	1.2e-06	0.00016
CHD4	mut	CTCF	mut	1.3e-06	0.00017
LRP1B	loss	CDKN2A	loss	1.5e-06	0.00021
GATA3	mut	PIK3CA	mut	1.7e-06	0.00023
KRAS	mut	PPP2R1A	mut	1.9e-06	0.00025
PARK2	loss	CDKN2B	loss	2e-06	0.00025
AKT3	gain	WHSC1L1	gain	2e-06	0.00025
SDCCAG8	gain	WHSC1L1	gain	2.1e-06	0.00026
ORAOV1	gain	CCNE1	gain	2.9e-06	0.00035
CCND1	gain	CCNE1	gain	2.9e-06	0.00035
MCL1	gain	WHSC1L1	gain	3.1e-06	0.00037
MDM4	gain	WHSC1L1	gain	3.2e-06	0.00037
ARID1A	mut	ARHGAP35	mut	3.2e-06	0.00037
CCND1	gain	ING1	gain	3.7e-06	0.00041
ORAOV1	gain	ING1	gain	3.7e-06	0.00041
SIN3A	mut	CTCF	mut	3.7e-06	0.00041
MDM4	gain	MYC	gain	4.3e-06	0.00048
KRAS	mut	MLLT4	mut	4.4e-06	0.00048
RBFOX1	loss	CSMD1	loss	4.7e-06	0.0005
ARID5B	mut	PPP2R1A	mut	5e-06	0.00051
CEP170	gain	CCND1	gain	5e-06	0.00051
CEP170	gain	ORAOV1	gain	5e-06	0.00051
RB1	mut	CDKN2A	loss	5e-06	0.00051
PARK2	loss	CDKN2A	loss	5.6e-06	0.00057
NRAS	mut	KRAS	mut	6e-06	0.00059
AKR1C2	gain	CCND1	gain	6.1e-06	0.00059
AKR1C2	gain	ORAOV1	gain	6.1e-06	0.00059
KRAS	mut	SMARCA4	mut	6.4e-06	0.00061
NUMA1	mut	TP53	mut	6.4e-06	0.00061
PTEN	loss	WWOX	loss	8.1e-06	0.00077
TP53	mut	EP300	mut	8.2e-06	0.00077
MTOR	mut	TP53	mut	8.5e-06	0.0008
RB1	mut	CDKN2B	loss	8.9e-06	0.00081
ASPM	mut	CTNNB1	mut	8.9e-06	0.00081
PARK2	loss	CSMD1	loss	9.7e-06	0.00088
KRAS	mut	KALRN	mut	9.7e-06	0.00088
PTEN	loss	PIK3CA	mut	1.1e-05	0.00095

CCND1	gain	BCL2L1	gain	1.1e-05	0.00096
ORAOV1	gain	BCL2L1	gain	1.1e-05	0.00096
ORAOV1	gain	IRS2	gain	1.1e-05	0.00097
CCND1	gain	IRS2	gain	1.1e-05	0.00097
KRAS	mut	EP300	mut	1.3e-05	0.0012
CHD8	mut	TP53	mut	1.3e-05	0.0012
AKT3	gain	ERBB2	gain	1.4e-05	0.0012
AKT3	gain	CCND1	gain	1.4e-05	0.0012
AKT3	gain	ORAOV1	gain	1.4e-05	0.0012
SDCCAG8	gain	ERBB2	gain	1.4e-05	0.0012
SDCCAG8	gain	ORAOV1	gain	1.5e-05	0.0012
SDCCAG8	gain	CCND1	gain	1.5e-05	0.0012
PTEN	loss	PDE4D	loss	1.6e-05	0.0013
CHL1	loss	CDKN2A	loss	1.6e-05	0.0013
CNTN6	loss	CDKN2A	loss	1.6e-05	0.0013
KRAS	mut	ATR	mut	1.7e-05	0.0014
CEP170	gain	ERBB2	gain	1.8e-05	0.0014
CHL1	loss	CDKN2B	loss	1.8e-05	0.0014
CNTN6	loss	CDKN2B	loss	1.8e-05	0.0014
CTCF	mut	ERBB2	mut	1.9e-05	0.0015
CSMD1	loss	PTPRD	loss	2.1e-05	0.0015
CTNNB1	mut	DMD	mut	2.1e-05	0.0015
CCND1	gain	MYC	gain	2.1e-05	0.0015
ORAOV1	gain	MYC	gain	2.1e-05	0.0015
KRAS	mut	PIK3CG	mut	2.1e-05	0.0015
CTNNB1	mut	ATRX	mut	2.1e-05	0.0016
CTCF	mut	CTNNB1	mut	2.3e-05	0.0017
MCL1	gain	ORAOV1	gain	2.3e-05	0.0017
MCL1	gain	CCND1	gain	2.3e-05	0.0017
TP53BP1	mut	TP53	mut	2.4e-05	0.0017
PTEN	loss	DMD	loss	2.6e-05	0.0018
CTNNB1	mut	MLL3	mut	2.6e-05	0.0019
TP53	mut	CASP8	mut	2.6e-05	0.0019
CNTN4	loss	PTPRD	loss	3e-05	0.0022
PIK3CA	mut	BCOR	mut	3.1e-05	0.0022
KRAS	mut	PIK3R1	mut	3.4e-05	0.0024
CTNNB1	mut	ABCB1	mut	3.4e-05	0.0024
PTEN	mut	ERBB2	gain	3.5e-05	0.0025
CNTN4	loss	CDKN2A	loss	3.5e-05	0.0025
CNTN4	loss	CSMD1	loss	4.1e-05	0.0029
ARID1A	mut	PIK3CA	mut	4.1e-05	0.0029

FHIT	loss	CDKN2A	loss	4.2e-05	0.0029
KRAS	mut	CDK12	mut	4.2e-05	0.0029
PIK3CA	mut	FBXW7	mut	4.3e-05	0.0029
CNTN4	loss	CDKN2B	loss	4.3e-05	0.0029
KRAS	mut	LIFR	mut	4.5e-05	0.003
CNTN6	loss	CSMD1	loss	4.5e-05	0.003
CHL1	loss	CSMD1	loss	4.5e-05	0.003
KRAS	mut	ARHGAP35	mut	4.5e-05	0.003
TP53	mut	HUWE1	mut	4.5e-05	0.003
KRAS	mut	FN1	mut	4.7e-05	0.003
KRAS	mut	NF1	mut	4.7e-05	0.003
LRP1B	loss	CSMD1	loss	4.7e-05	0.003
TP53	mut	MAP3K4	mut	4.9e-05	0.0032
PDE4D	loss	CDKN2A	loss	5e-05	0.0032
CTNNB1	mut	RASA1	mut	5.1e-05	0.0033
CTCF	mut	RBMX	mut	5.4e-05	0.0034
FHIT	loss	CDKN2B	loss	5.4e-05	0.0034
KRAS	mut	MLL3	mut	5.5e-05	0.0035
TP53	mut	NSD1	mut	5.7e-05	0.0035
WWOX	loss	PARK2	loss	5.9e-05	0.0037
FN1	mut	CTNNB1	mut	6e-05	0.0037
CTCF	mut	TRIO	mut	6.1e-05	0.0038
KRAS	mut	MDC1	mut	6.1e-05	0.0038
KRAS	mut	DICER1	mut	6.3e-05	0.0039
KRAS	mut	DMD	mut	6.5e-05	0.004
CTNNB1	mut	TAF1	mut	6.6e-05	0.004
ERBB2	gain	WHSC1L1	gain	6.6e-05	0.004
SMC3	mut	KRAS	mut	6.9e-05	0.0041
PDE4D	loss	CDKN2B	loss	6.9e-05	0.0041
SLC16A1	loss	CSMD1	loss	6.9e-05	0.0041
CTCF	mut	TAF1	mut	7e-05	0.0042
TP53	mut	BCOR	mut	7.4e-05	0.0044
TP53	mut	PIK3CB	mut	7.5e-05	0.0044
MDM4	gain	MDM2	gain	7.7e-05	0.0045
NRAS	mut	RNF43	mut	8e-05	0.0047
AGAP2	gain	CDKN2A	loss	8.1e-05	0.0047
KRAS	mut	ESR1	mut	8.2e-05	0.0048
WWOX	loss	MAP2K4	loss	8.3e-05	0.0048
RB1	loss	LRP1B	loss	8.4e-05	0.0048
MDM4	gain	KAT6A	gain	9e-05	0.0052
COL18A1	mut	PIK3CA	mut	9e-05	0.0052

CCND1	mut	MECOM	mut	9.3e-05	0.0053
CEP170	gain	KAT6A	gain	9.7e-05	0.0056
PPP2R1A	mut	RBMX	mut	0.0001	0.0058
TPR	mut	CTNNB1	mut	0.00011	0.0064
KRAS	mut	EGFR	mut	0.00011	0.0065
CTCF	mut	CIC	mut	0.00012	0.0066
CHD4	mut	CTNNB1	mut	0.00012	0.0068
CDKN2A	loss	DMD	loss	0.00012	0.0068
TPR	mut	KRAS	mut	0.00012	0.0068
CHL1	loss	PTPRD	loss	0.00012	0.0069
CNTN6	loss	PTPRD	loss	0.00012	0.0069
CBFB	mut	TP53	mut	0.00013	0.0071
KRAS	mut	FOXA2	mut	0.00013	0.0071
MDM4	gain	EGFR	gain	0.00013	0.0074
GATA3	mut	CDH1	mut	0.00013	0.0075
ARID5B	mut	FOXA2	mut	0.00014	0.0075
ATM	mut	CTCF	mut	0.00014	0.0077
MTOR	mut	KRAS	mut	0.00014	0.0079
AGAP2	gain	CDKN2B	loss	0.00016	0.0088
NFE2L2	mut	GNAS	mut	0.00017	0.0093
CTNNB1	mut	APC	mut	0.00017	0.0093
TP53	mut	ADCY1	mut	0.00017	0.0093
KRAS	mut	PRPF8	mut	0.00017	0.0093
NRAS	mut	AXIN2	mut	0.00017	0.0095
MCL1	gain	PIK3CA	mut	0.00018	0.0096
KRAS	mut	AMPH	mut	0.00018	0.0098
PTEN	loss	FHIT	loss	0.00018	0.0098
PIK3CA	mut	MYC	gain	0.00018	0.0099

Supplemental text

Parameter estimation

To apply the DISCOVER test, we need estimates of the alteration probabilities p_{ij} for all genes i and all tumors j. These estimates are used as parameters of the Poisson-Binomial distribution used by the test. Here, we show that each alteration probability can be written in terms of two parameters.

$$p_{ij} = \frac{1}{1 + e^{\mu_i + \lambda_j}}$$

For estimating the parameters of the Poisson-Binomial distribution we maximize the information entropy (or equivalently below, minimize the negative of the entropy), subject to the constraints that the expected row and column marginals match the observed ones.

$$\begin{aligned}
\min_{p} \quad & \sum_{i=1}^{n}\sum_{j=1}^{m} p_{ij}\log p_{ij} + (1-p_{ij})\log(1-p_{ij}) \\
\text{s.t.} \quad & \\
& \sum_{j=1}^{m} p_{ij} = R_i && , \quad 1 \le i \le n \\
& \sum_{i=1}^{n} p_{ij} = C_j && , \quad 1 \le j \le m \\
& 0 \le p_{ij} \le 1 && , \quad 1 \le i \le n, 1 \le j \le m
\end{aligned}$$

where

$$\begin{aligned}
R_i &= \sum_{j=1}^{m} x_{ij} \\
C_j &= \sum_{i=1}^{n} x_{ij}
\end{aligned}$$

We first turn this constrained optimization problem into an unconstrained one by defining the Lagrangian dual. The Lagrangian is as follows.

$$\begin{aligned}
\mathcal{L}(p,\mu,\lambda) = \sum_{i,j} p_{ij}\log p_{ij} + (1-p_{ij})\log(1-p_{ij}) + \sum_i \mu_i(\sum_j p_{ij} - R_i) \\
+ \sum_j \lambda_j(\sum_i p_{ij} - C_j)
\end{aligned}$$

which we rewrite to

$$\mathcal{L}(p,\mu,\lambda) = \sum_{i,j} p_{ij}\log p_{ij} + (1-p_{ij})\log(1-p_{ij}) + \sum_i \mu_i \sum_j p_{ij} - \sum_i \mu_i R_i + \sum_j \lambda_j \sum_i p_{ij} - \sum_j \lambda_j C_j$$

We then optimize the Lagrangian with respect to the variables p_{ij} by setting the partial derivatives to 0 and solving for those variables.

$$\frac{\partial \mathcal{L}}{\partial p_{ij}} = \log p_{ij} - \log(1-p_{ij}) + \mu_i + \lambda_j = 0$$

From this, we derive that

$$\log \frac{p_{ij}}{1-p_{ij}} = -\mu_i - \lambda_j$$

The left-hand side of this equation is the familiar logit function, the inverse of which is the logistic function. Hence, we obtain the following expression for p_{ij}.

$$p_{ij} = \frac{1}{1+e^{\mu_i+\lambda_j}}$$

With this, we can formulate the Lagrangian dual as follows.

$$\max_{\mu,\lambda} \sum_{i,j} p_{ij}\log p_{ij} + (1-p_{ij})\log(1-p_{ij}) + \sum_i \mu_i(\sum_j p_{ij} - R_i) + \sum_j \lambda_j(\sum_i p_{ij} - C_j)$$

where p_{ij} is defined as above.